UWB System for Time-Domain Near-Field Antenna Measurement

B. Levitas[#1], M. Drozdov[#], I. Naidionova[#], S. Jefremov[#], S. Malyshev[*2], A. Chizh[*3]

www.geozondas.com

[#] *Geozondas Ltd.,*

16, Shevchenko Str., LT-03111, Vilnius, Lithuania

[1]levitas@geozondas.com

[*]*Lab. of Semiconductor Optoelectronics, Stepanov Institute of Physics*

22, Logoiski trakt, 220090, Minsk, Belarus

[2]malyshev@ieee.org, [2]chizh@ieee.org

***Abstract*—An UWB system for time-domain near-field antenna measurements with new time-domain data pre-processing algorithms has been proposed. UWB system developed is suitable for planar, cylindrical, and spherical near-field antenna measurements. It is shown that near-field time-domain measurements using developed UWB system with optically-fed antenna probe are in a good agreement with conventional far-field antenna measurements.**

I. Introduction

The main advantage of time-domain antenna measurements is the possibility to characterize antenna in the ordinary laboratory room without usage of anechoic chamber [1]. To avoid data corruption during time-domain antenna measurements it is enough to ensure, that reflections from surrounding objects are outside of measurement time window. However, outdoor test ranges are usually used for large antennas, because their far field zone starts far from aperture. Other possibility to measure such antennas is to use near-field measurement setups. Near-field measurements can be carried out not only in frequency domain, but in time domain also [2],[3]. In this paper UWB system for time-domain near-field antenna measurements with new time-domain data pre-processing algorithms and optically-fed antenna probe has been proposed.

II. UWB System

In near-field time-domain measurements a short UWB pulse is used as a test signal and digital UWB sampling oscilloscope is used as receiver (Fig. 1). The signal received by sampling receiver is pre-processed to correct hardware time drift and change of delay of time window. After Fourier transform of signal all well-known frequency domain algorithms can be used for further data processing [4]-[6].

There are three main near-field measurement methods: planar, cylindrical and spherical. The equipment for all three setups is almost the same, naturally there is only difference in positioning devices used. For planar near-field measurements system XY scanner is used (Fig. 2), for cylindrical measurements vertical scanner and azimuth positioner are used (Fig. 3), and for spherical measurements azimuth and elevation positioner is used (Fig. 4). The difference is that in cylindrical measurements antenna under test (AUT) is positioned on foam holder and rotated, and antenna probe is moved only along vertical axis. For spherical near-field measurements a 2D positioner with foam AUT holder and coinciding azimuth and elevation centrums of rotation was developed. Sampling oscilloscope with sampling head in time-domain measurements is counterpart of network analyzer in frequency-domain measurements. To speed up measurements pulse repetition rate of pulse generator and sampling converter was increased up to 7 MHz. Antenna can be measured in frequency band 1–20 GHz.

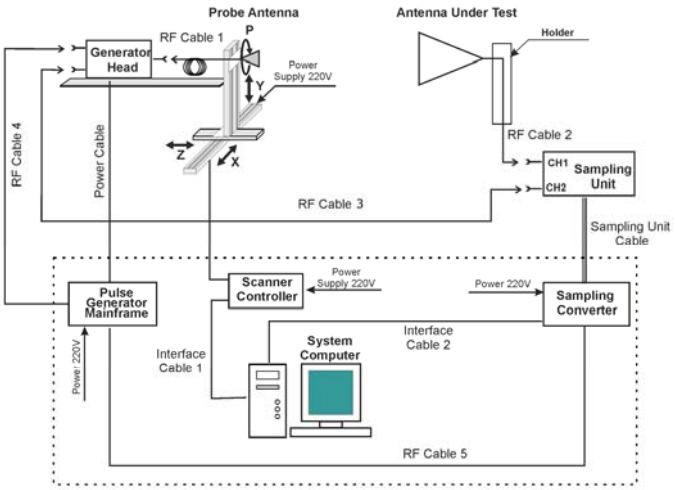

Fig. 1. Planar time-domain near-field antenna measurement scheme

The main advantage of the time-domain near-field antenna measurements is the possibility to measure antennas without anechoic chamber. Moreover, the hardware is cheaper and the measurement linearity is better in comparison to the frequency-domain method. On the other hand, the time-domain near-field antenna measurements have smaller dynamic range and higher frequency base error in comparison to the frequency-domain method.

One of the problems in realization of time-domain near-field antenna measurement scheme is a hardware time drift, which is equivalent to positioning error in near-field measurements. There are several sources of time drift in time-domain measurements and different ways to decrease or

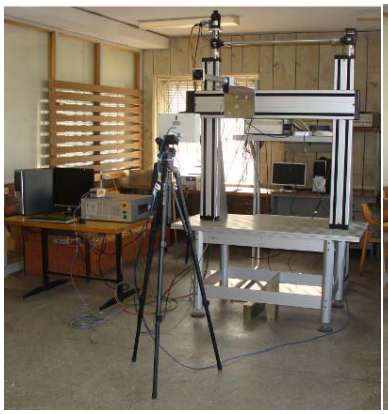

Fig. 2. Planar time-domain near-field antenna measurement setup

Fig. 3. Cylindrical time-domain near-field antenna measurement setup

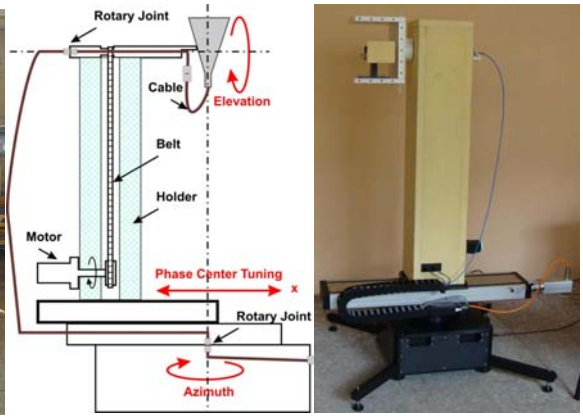

Fig. 4. Scheme (left) and photo (rigth) of azimuth and elevation positioner used for spherical near-field antenna measurements

remove it entirely. First source of time drift is bending of cables. At least one cable (RF cable 1 in Fig.1) is not stationary during near-field scan, so measurement errors arise because of cable movements. To eliminate such time drift it is necessary to use phase stable RF cables or optically-fed probe antennas [7]. It is worth noting that for spherical measurements it is possible to realize measurement setup without RF cables movements using positioner with rotary joints. To correct time drift of pulse generator and sampling receiver an RF cable (RF cable 3 in Fig.1) is added into the measurement setup. That kind of time drift is very slow but is accumulated during long measurements. To eliminate its impact on measurement results it is necessary to perform pre-processing drift correction. Two pulses are generated by pulse generator without time drift between them because of the reference pulse is a branching of main. At the receiver there is zero drift between channels because of common sampling pulse. Using those properties time drift in the main measurement channel can be corrected by control of signal position shift in reference channel. Signal phase correction proceeds through processing of the reference signal, measurement of the time drift, and phase correction.

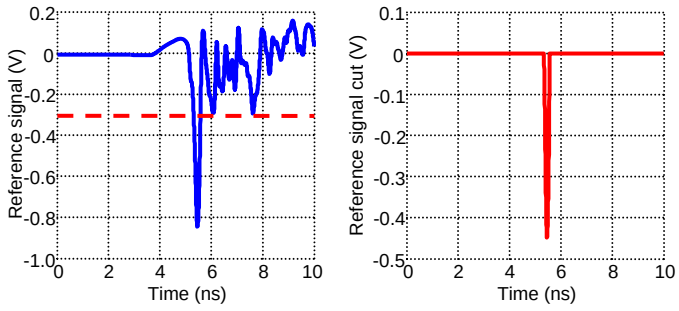

Fig. 5. Signals in reference channel

Processing includes low pass filtering and pulse cutting. After cutting a convenient form of pulse is obtained. To have clear correlation function of two reference signals in further steps of algorithm, threshold is used to obtain only part of signal as shown in Fig. 5. During near-field scan the shape of reference signal cut doesn't change. After each acquisition correlation function R_{1m} of first signal cut s_1 with current signal cut s_m is calculated:

$$R_{1m}(t) = IFFT\left(FFT(s_1) \otimes FFT^*(s_m)\right), \quad (1)$$

where FFT and IFFT denote Fast Fourier Transform and Inverse Fast Fourier Transform accordingly.

Signal time drift τ_m is equal to shift of correlation function R_{1m} maximum. To receive resolution better than signal sampling step a parabolic approximation of correlation function top is carried out. Phase of pulse obtained in measurement channel is corrected using calculated drift value. The result resolution is about 0.1 of sampling step. To shift the signal in measurement channel by time lesser than sampling step its spectrum in frequency domain is calculated using the following formula:

$$\tilde{s}_m[n] = s_m[n] e^{-i2\pi n \tau_m / N}, \; n = \overline{1 \ldots N}, \quad (2)$$

where N is the total number of sample points, τ_m is time drift calculated by means of (1) for each point.

Sliding windowing function is used as one of pre-processing steps. During planar and cylindrical near field scan the delay of received pulse is changing. Delay of sliding windowing function must be changed accordingly, as shown in Fig. 6. Minimum time window duration depends on shape of spectrum of received signal. It can be shown, that when frequency response has a step, after time-domain measurement slope duration $\Delta f > 1 / T$. As result, minimum duration of windowing function:

$$T_{\min} = 1/\Delta f_1 + 1/\Delta f_2, \quad (3)$$

where Δf_1 and Δf_2 are slope durations of the beginning and the end of the receiving signal band pass accordingly.

It is known [4], that minimum distance between antenna probe and AUT must be larger than $3\lambda_{max}$, where λ_{max} is the maximum wavelength of measurement bandwidth. There will be no reflections in time window if $T < 6\lambda_{max}/c$. Taking in account formula (3), the following inequality for time window can be obtained:

$$1/\Delta f_1 + 1/\Delta f_2 < T < 6\,\lambda_{max}/c\,, \qquad (4)$$

It is worth noting that for narrow band signal the requirements (4) are unrealizable.

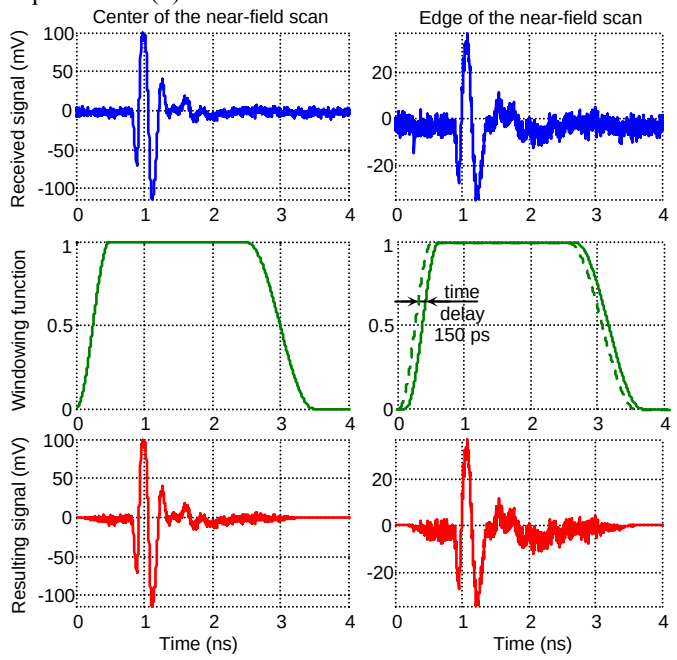

Fig. 6. Usage of windowing function in time-domain near-field measurements

For measurement error estimation the comparison with far field measurement results is used. Fig. 7 shows comparison of double ridged TEM horn antenna GZ0126DRH radiation pattern obtained from far-field and cylindrical near-field measurements. The difference in vicinity of 180° is caused by influence of vertical feed cable in far field. In near field this influence is out of time window.

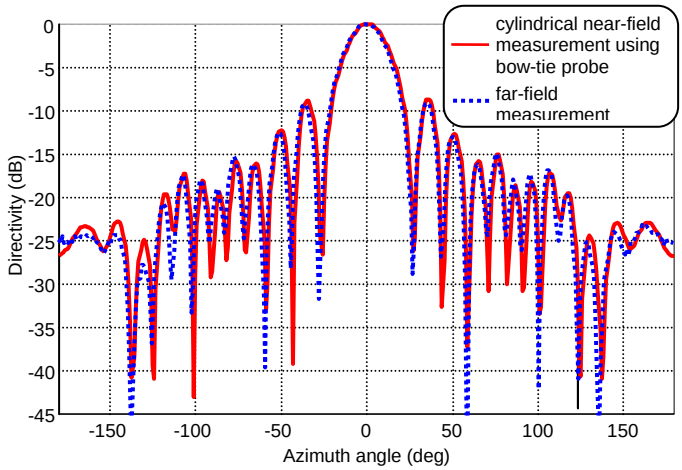

Fig. 7. Comparison of double ridged TEM horn antenna radiation patterns (H-plane) obtained by means of far-field measurements and cylindrical near-field measurements at the frequency 6 GHz

III. Optically-fed UWB Probe

Many factors which have a great influence on the accuracy of the results of the near-field antenna measurements, are connected with the measuring probe itself [8]. Among them, the most important are the errors of probe positioning, probe relative radiation pattern and polarization properties. The usage of fiber-optic cable with optically-fed probe instead of coaxial cable with conventional antenna probe allows to eliminate the dependence of radiation pattern on fed cables position and mutual coupling of the probe with its feeder [9].

The block diagram for optoelectronic generation of UWB pulse is shown in Fig. 8. Pulse generator GZ1117 (Geozondas Ltd.) emits negative Gaussian-like pulse with amplitude of 40 V and full width at half maximum of 110 ps. Electrical pulse switches the pigtailed laser diode from a state below threshold into inversion, and the laser generally emits several relaxation oscillations. Under proper width and amplitude of the input electrical pulse, it is possible to extract a first optical spike in the relaxation oscillations, so that the waveform of the output optical pulse is determined by the photon lifetime in the laser diode cavity. By adjusting the amplitude of the input electrical Gaussian pulse to 19 V the laser diode module emits single optical pulse with amplitude of 25 mW and full width at half maximum of 27 ps. For adjusting the amplitude of initial electrical pulse the variable attenuator has been used.

The pigtailed laser used is uncooled InGaAsP/InP multi quantum-well distributed-feedback laser with coaxial TO-package under zero bias condition. This laser has emission wavelength of 1311 nm, resonance frequency higher than 11 GHz, and side-mode suppression ratio higher than 50 dB. The single mode fiber-optic cable is used to transmit short optical pulse to the UWB probe, which emits the UWB pulse.

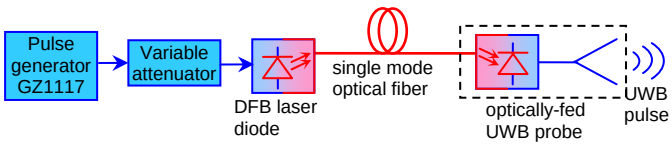

Fig. 8. Optoelectronic UWB pulse generation scheme

Fig. 9 shows prototype of the optically-fed UWB probe for time-domain near-field antenna measurements. Optically-fed UWB probe developed is based on pigtailed photodiode integrated with bow-tie radiator. The dimensions of the bow-tie radiator are 30×30×1 mm. The photodiode is soldered onto the backside of the antenna. The bias voltage is supplied to the photodiode through two 100 Ω resistors, soldered at the both edges of bow-tie radiator. Since reverse-biased photodiode consumes a very low electrical power the two 1.5 V batteries have been used in series as power supply.

Fig. 9. Optically-fed UWB probe prototype

The pigtailed photodiode used in the UWB probe is InGaAs/InP p-i-n photodiode with coaxial TO-package. The photodiode has a sensitive area diameter of 40 μm, spectral sensitivity range of 850–1650 nm, and 3dB-bandwidth of 6 GHz. For coupling of the photodiode with single mode optical fiber the tapered fiber lens has been used. To achieve high coupling efficiency the active fiber alignment and index matching resin between the diode and the fiber lens has been used. This results in high responsivity of the pigtailed photodiode (1 A/W @ 1310 nm), which ensure low optoelectronic conversion loss in the UWB probe.

The maximum amplitude of the generated UWB pulse is limited by maximal photocurrent generated by the photodiode, which is usually not more than tens of milliamperes. Thus using this technique it is possible to generated UWB pulse with amplitude not more than several volts, which is sufficient for most UWB applications. Fig. 10 shows antenna pattern at the frequency 4 GHz of the optically-fed UWB probe and temporal waveform of the UWB pulse generated. One can see that optically-fed UWB probe has uniform radiation pattern within angle range of ±40º, while conventional bow-tie antenna fed by coaxial cable through SMA connector has uniform radiation pattern within only ±15º.

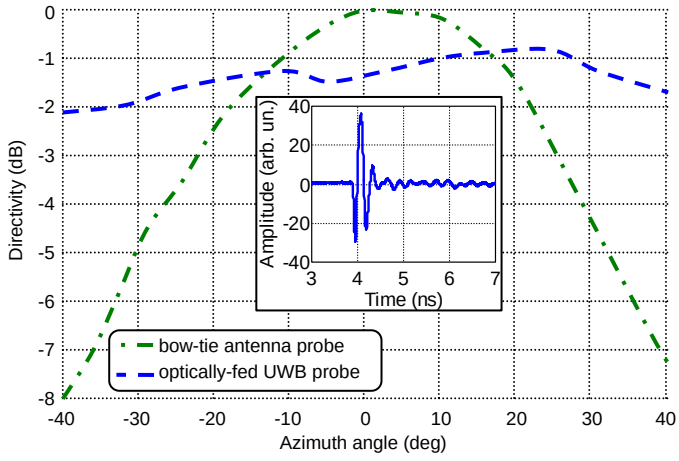

Fig. 10. Radiation patterns (H-plane) of the optically-fed UWB probe and bow-tie antenna probe for near-field antenna measurements at the frequency 4 GHz. The inset shows measured temporal waveform of the UWB pulse generated by the optically-fed UWB probe

Fig. 11 shows radiation patterns of the ridged horn antenna P6-23 measured in far field and in near filed using optically-fed UWB probe and conventional bow-tie antenna fed by coaxial cable. The planar near-field scanning square was 1 ×1 m, and distance between scanning plane and antenna under test was 60 cm. The figure shows that differences between measurements in far field and in near field is much less in the case of usage of the optically-fed UWB probe. One can see that errors in the near-filed measurements using conventional bow-tie antenna fed by coaxial cable significantly increase for the angles more than 15º. Thus, optically-fed UWB probe developed allows to carry out time-domain near-field antenna measurements with high accuracy. It should be noted that ripples for measurements with optically-fed UWB probe are caused by Gibbs phenomenon due to scan plane limitation (1 x 1 m).

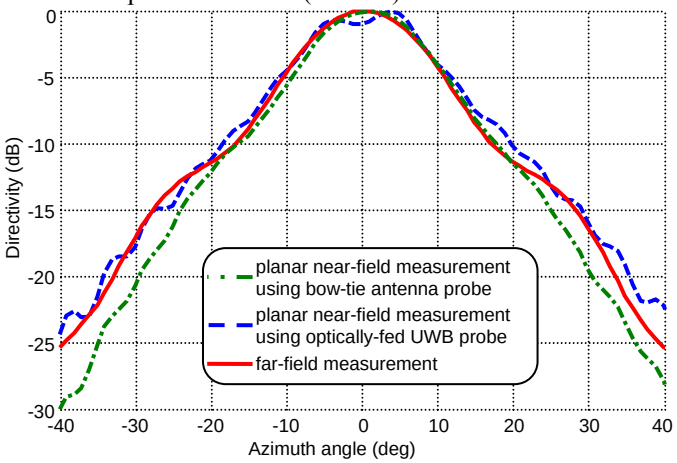

Fig. 11. Ridged horn antenna P6-23 radiation pattern (H-plane) obtained by means of far-field measurements and planar near-field measurements at the frequency 4 GHz using two different probes

IV. Conclusions

Time-domain near-field antenna measurement system operating in the frequency range of 1–20 GHz has been developed. UWB system for time-domain near-field antenna measurements includes novel pulse generator and sampling receiver with 7 MHz pulse repetition rate, positioner with coinciding azimuth and elevation centrums of rotation, and optically-fed UWB probe. Antenna measurements can be carried out in planar, cylindrical and spherical surface without usage of anechoic chamber. Hardware time drift correction algorithms have been presented. Requirements for time window duration are calculated based on AUT frequency response slope. It is shown that time-domain near-field antenna measurements are in a good agreement with far-field antenna measurements.

References

[1] B. Levitas, D. Ponomarev, “Antenna measurements in time domain”, *Proc. of IEEE Antenna and Propagation Society International Symposium*, pp.573–576, vol. 1, Jul. 1996.

[2] T. Hansen, A. Yaghjian, “Planar near-field scanning in the time domain”, *IEEE Transactions on Antennas and Propagation*, vol.42, n.9, pp.1280–1300, Sep. 1994

[3] T. Hansen, “Formulation of spherical near-field scanning for electromagnetic fields in the time domain”, *IEEE Transactions on Antennas and Propagation*, vol.45, n.4, pp.620–630, Apr. 1997

[4] C. Balanis, *Antenna theory. Analysis and design*, 2nd ed., 1997

[5] W. Leach Jr., D. Paris, "Probe compensated near-field measurements on a cylinder," *IEEE Transactions on Antennas and Propagation*, vol.21, n.4, pp.435–445, Apr. 1973

[6] J.E. Hansen, *Spherical near-field antenna measurements*, London, 1998

[7] Y. Yashchyshyn, J. Modelski, S. Malyshev, A. Chizh, M. Svirid, P. Wegrzyniak, "Near field antennas measurements using photonic antenna," *Proc. EuMC'07*, pp. 576–579, Oct. 2007.

[8] T. Hansen, A. Yaghjian, "Formulation of probe-corrected planar near-field scanning in the time domain", *IEEE Transactions on Antennas and Propagation*, vol.43, n.6, pp.569–584, Jun. 1995

[9] A. Chizh, S. Malyshev, S. Jefremov, B. Levitas, I. Naidionova, "Impulse transmitting photonic antenna for ultra-wideband applications", *Proc. of MIKON'10*, pp. 346–348, June 2010.